nature communications

Article

https://doi.org/10.1038/s41467-024-52822-4

Elucidating the molecular logic of a metabotropic glutamate receptor heterodimer

Received: 2 January 2024

Accepted: 20 September 2024

Published online: 03 October 2024

Check for updates

Xin Lin[1,2], Davide Provasi[3], Colleen M. Niswender[4,5,6,7,8], Wesley B. Asher[1,2] & Jonathan A. Javitch[1,2,9]

Metabotropic glutamate (mGlu) receptor protomers can heterodimerize, leading to different pharmacology compared to their homodimeric counterparts. Here, we use complemented donor-acceptor resonance energy transfer (CODA-RET) technology that distinguishes signaling from defined mGlu heterodimers or homodimers, together with targeted mutagenesis of receptor protomers and computational docking, to elucidate the mechanism of activation and differential pharmacology in $mGlu_{2/4}$ heteromers. We demonstrate that positive allosteric modulators (PAMs) that bind an upper allosteric pocket in the $mGlu_4$ transmembrane domain are active at both $mGlu_{4/4}$ homomers and $mGlu_{2/4}$ heteromers, while those that bind a lower allosteric pocket within the same domain are efficacious in homomers but not heteromers. We further demonstrate that both protomers of $mGlu_{2/4}$ heteromers are cis-activated by their orthosteric agonists, signaling independently with no trans-activation detected. Intriguingly, however, upper pocket $mGlu_4$ PAMs enable trans-activation in $mGlu_{2/4}$ heteromers from $mGlu_4$ to the $mGlu_2$ protomer and also enhance cis-activation of the $mGlu_2$ protomer. While $mGlu_2$ PAMs enhanced $mGlu_2$ cis-activation in the heterodimer, we were unable to detect trans-activation in the opposite direction from $mGlu_2$ to the $mGlu_4$ protomer, suggesting an asymmetry of signaling. These insights into the molecular logic of this receptor heteromer are critical to building toward precision targeted therapies for multiple neuropsychiatric disorders.

Glutamate, the major excitatory neurotransmitter in the mammalian central nervous system, acts at both ionotropic and metabotropic glutamate (mGlu) receptors, the latter being members of the class C G protein-coupled receptor (GPCR) family. Glutamate activates these receptors to modulate neuronal excitability and synaptic transmission throughout the brain[1]. Several studies have suggested that mGlu receptors are promising targets for therapeutics of a variety of neuropsychiatric disorders, including Alzheimer's disease[2], Parkinson's disease[3,4], depression and stress-related disorders[5,6], as well as schizophrenia[7,8].

[1]Department of Psychiatry, Vagelos College of Physicians and Surgeons, Columbia University, New York, NY, USA. [2]Division of Molecular Therapeutics, New York State Psychiatric Institute, New York, NY, USA. [3]Department of Pharmacological Sciences, Icahn School of Medicine at Mount Sinai, New York, NY, USA. [4]Department of Pharmacology, Vanderbilt University, Nashville, TN, USA. [5]Warren Center for Neuroscience Drug Discovery, Vanderbilt University, Nashville, TN, USA. [6]Vanderbilt Kennedy Center, Vanderbilt University Medical Center, Nashville, TN, USA. [7]Vanderbilt Brain Institute, Vanderbilt University, Nashville, TN, USA. [8]Vanderbilt Institute for Chemical Biology, Vanderbilt University, Nashville, TN, USA. [9]Department of Molecular Pharmacology and Therapeutics, Vagelos College of Physicians and Surgeons, Columbia University, New York, NY, USA. e-mail: wesley.asher@nyspi.columbia.edu; jonathan.javitch@nyspi.columbia.edu

There are eight mGlu receptor subtypes, divided into three major groups based on sequence similarity, G protein coupling, and shared pharmacology. Group I ($mGlu_1$ and $mGlu_5$) receptors predominantly couple to G_q/G_{11}, whereas groups II ($mGlu_2$ and $mGlu_3$) and III ($mGlu_4$, $mGlu_6$, $mGlu_7$, and $mGlu_8$) receptors are predominantly coupled to G_i/G_o[1,9]. The mGlu receptors form stable, disulfide-linked dimers in the endoplasmic reticulum that are trafficked to the plasma membrane[10,11]. Each mGlu receptor protomer is composed of a large amino-terminal venus flytrap domain (VFD), which contains the orthosteric ligand-binding site for glutamate[1,12]. Agonist binding within the VFDs induces structural changes that are propagated via the cysteine-rich domains to the seven transmembrane domains (7TM), leading to G protein binding and activation.

In addition to forming homodimers, mGlu protomers also can heterodimerize, both in heterologous cells[13,14] and in the brain[15–20]. When co-expressed in heterologous cells, group I mGlu receptor protomers can form heterodimers with each other, and group II and III protomers can form heterodimers within and between groups[13,21]. Importantly, heterodimerization can have dramatic effects on receptor pharmacology[17–20]. As mGlu receptor subtypes are expressed heterogeneously throughout a myriad of brain circuits, the significance of mGlu receptor heterodimerization on cellular physiology and pharmacology has emerged as a critical question for the mGlu receptor field, fueling the hope for precision medicine approaches, wherein specific circuits might be selectively targeted for therapeutic purposes by mGlu heterodimer-selective therapies, which have not yet been reported.

Much of the work to date on mGlu receptor heterodimers has focused on $mGlu_{2/4}$ heteromers, both in heterologous cells[17] and in the cortex and striatum[18,19]. More recently, direct evidence for these heteromers in several brain regions in mice, including the prefrontal cortex, striatum, hippocampus, and olfactory bulb, has been provided by energy transfer between labeled nanobodies that specifically bind endogenous $mGlu_2$ and $mGlu_4$ protomers[15]. Electrophysiological studies of select $mGlu_4$ positive allosteric modulators (PAMs), such as the structurally similar VU0155041[18] and Lu AF21934, have shown that while these ligands potentiate responses at corticostriatal synapses[22], other $mGlu_4$ PAMs, such as PHCCC[18], cannot. Similar results were also observed at thalamocortical synapses, where Lu AF21934 potentiated responses, but PHCCC and another $mGlu_4$ PAM, VU0418506, were inactive. Interestingly, however, both Lu AF21934 and PHCCC show PAM effects at other synapses, including the striatopallidal synapse[23,24]. We hypothesized that differential PAM activity at $mGlu_{4/4}$ homomers and $mGlu_{2/4}$ heterodimers might underlie these divergent electrophysiology results.

While this hypothesis regarding the potential function and unique pharmacology of heterodimers versus homodimers is intriguing, determining whether putative heterodimers can signal and defining their pharmacological properties relative to their corresponding homodimers is complex, as co-expression of $mGlu_2$ and $mGlu_4$ protomers could lead to a mixed population of $mGlu_{2/2}$ and $mGlu_{4/4}$ homodimers as well as $mGlu_{2/4}$ heterodimers at the cell surface. Traditional signaling assays where mGlu receptor protomer assembly and expression is not specifically controlled via receptor engineering cannot distinguish between these different combinations, making it virtually impossible to attribute specific function or pharmacology to a hetero- or homo-dimer pair.

To overcome this challenge, we developed complemented donor-acceptor resonance energy transfer (CODA-RET) to probe signaling from defined homodimers or heterodimers[25]. In this assay, a modified *Renilla reniformis* luciferase 8 (RLuc8) is split into N-terminal (L1) and C-terminal (L2) fragments that are nonfunctional when expressed alone, but, when brought into close proximity, complement to form a functional luciferase[26,27]. To isolate signaling from defined homo- or heterodimers, these RLuc8 fragments are fused to the C termini of $mGlu_2$ and/or $mGlu_4$ protomers, allowing control over the complemented species. By monitoring bioluminescence resonance energy transfer (BRET) between the complemented fragments of RLuc8 as donor and monomeric Venus (mVenus) fused to the $G\alpha_i$ subunit as acceptor, we can selectively measure recruitment of G protein by defined homodimers or heterodimers in response to receptor activation. Importantly, mGlu homodimers formed by two protomers fused to L1 or L2 alone cannot form complemented RLuc8 and thus are optically silent in this assay.

Intrigued by the differential effects of Lu AF21934 and VU0418506 at various synaptic locations, we previously investigated the effects of these PAMs in our CODA-RET assay and showed that, while both compounds showed similar PAM effects at $mGlu_{4/4}$ homodimers, Lu AF21934 acted as a PAM at $mGlu_{2/4}$ heterodimers whereas VU0418506 had no effect[16]. These experiments mirrored the profile observed in our and others' electrophysiology experiments and unambiguously demonstrated that an $mGlu_4$ PAM can be active at $mGlu_{4/4}$ homomers, but inactive at $mGlu_{2/4}$ heterodimers, consistent with our hypothesis described above. However, the molecular determinants of these differences in activity remained a complete mystery. Likewise, whether other $mGlu_4$ PAMs, including VU0155041 and PHCCC, also show similar differential activity in our CODA-RET assay, has yet to be determined, and could provide valuable information related to the molecular logic of this differential pharmacology and heteromer function.

In this study, we use CODA-RET with targeted mutagenesis of receptor protomers and computational docking, as well as multiple $mGlu_4$ allosteric modulators, to dissect the mechanism of signaling and interprotomer interactions in both $mGlu_{4/4}$ homomers and $mGlu_{2/4}$ heteromers. We reveal that PAMs that bind in the lower part of the allosteric pocket in the $mGlu_4$ 7TM domain, while efficacious in $mGlu_{4/4}$ homomers, are inactive at $mGlu_{2/4}$ heteromers. In contrast, PAMs that bind in the upper pocket of the allosteric site are active at both $mGlu_{4/4}$ homomers and $mGlu_{2/4}$ heteromers. We also show that both protomers of the heteromer are cis-activated by their orthosteric agonists, signaling independently with no trans-activation observed. Remarkably, however, we go on to show that trans-activation between the $mGlu_4$ and $mGlu_2$ protomers is enabled in the presence of the upper pocket $mGlu_4$ PAMs. This work provides a deep mechanistic understanding of mGlu heterodimer activation and allosteric modulation that is critical to the development and discovery of heteromer-selective compounds and highlights the diversity of functional complexity within dimeric transmembrane protein receptors.

Results

$mGlu_4$ PAMs differentially affect $mGlu_{2/4}$ heterodimers

We first used CODA-RET in defined $mGlu_{4/4}$ homodimers to probe the actions of multiple $mGlu_4$-specific PAMs (Supplementary Fig. 1a). Both VU0155041 and PHCCC (Fig. 1a, b) enhanced activation of $mGlu_{4/4}$ homomers (Fig. 1c) by the $mGlu_4$ orthosteric agonist L-AP4 (Supplementary Fig. 1b), as evidenced by lower half maximal effective concentration (EC_{50}) and higher maximal effect (E_{max}) values relative to L-AP4 alone (Fig. 1d), confirming their reported activity as $mGlu_4$ PAMs[23,28,29]. When applied to defined $mGlu_{2/4}$ heterodimers using the same assay (Fig. 1e), VU0155041 still enhanced L-AP4-induced activation, whereas PHCCC had no effect (Fig. 1f). Two other $mGlu_4$ PAMs, VU0364770 and ADX88178, showed the same profile as PHCCC, as did the previously investigated VU0418506[16] (Supplementary Fig. 1c, d). Lu AF21934 also enhanced activation at both $mGlu_{2/4}$ heteromers and $mGlu_{4/4}$ homomers (Supplementary Fig. 1c, d), consistent with our previous findings[16]. Control experiments ruled out contributions from forced protomer association or bystander BRET that might contribute to our CODA-RET signal (Supplementary Fig. 2 and Note 1), validating that the observed signals in our assay originate from defined receptor homomers or heteromers. Taken together, these results reinforce our

https://doi.org/10.1038/s41467-024-52822-4

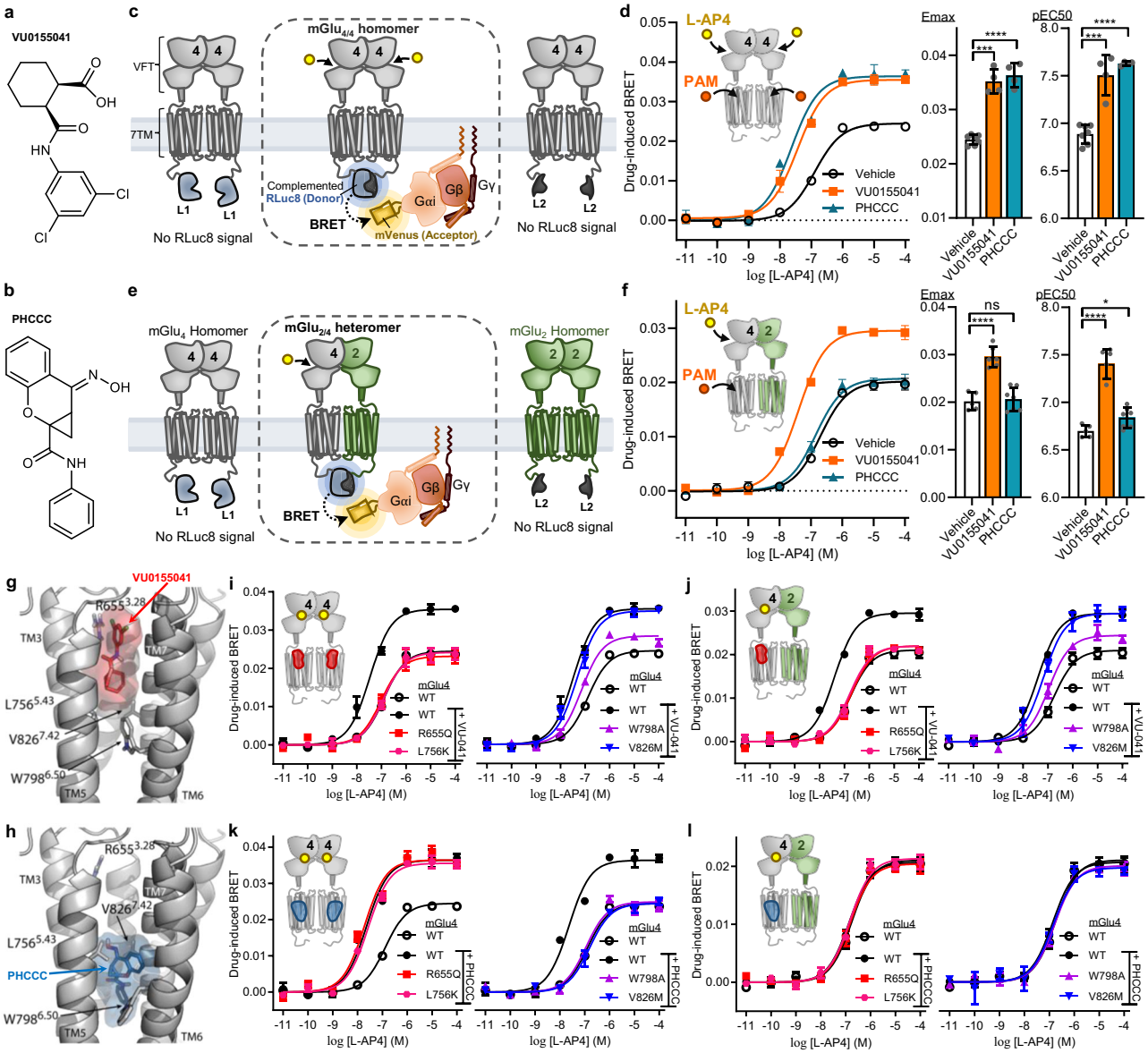

Fig. 1 | mGlu$_4$ PAMs that affect both mGlu$_{2/4}$ heterodimers and mGlu$_{4/4}$ homodimers bind an allosteric upper-binding pocket. a Structure of VU0155041. **b** Structure of PHCCC. **c** CODA-RET schematic in homodimer mode. **d** CODA-RET measurements with mGlu$_{4/4}$ homodimers showing (left) L-AP4-concentration-response curves in the absence (dimethyl sulfoxide (DMSO) vehicle) or presence of 50 μM PAMs (VU0155041 or PHCCC) and (right) corresponding E_{max} and pEC_{50} values. For E_{max} plot: $^{***}p = 1.2 \times 10^{-6}$; $^{****}p = 4.3 \times 10^{-7}$; For pEC_{50} plot: $^{***}p = 9.3 \times 10^{-5}$, $^{****}p = 1.7 \times 10^{-7}$; unpaired, two-tailed t-test. **e** CODA-RET schematic in heterodimer mode. **f** CODA-RET measurements with mGlu$_{2/4}$ heterodimers showing (left) L-AP4-concentration-response curves in the absence (DMSO vehicle) or presence of 50 μM PAMs (VU0155041 or PHCCC) and (right) corresponding E_{max} and pEC_{50} values. For E_{max} plot: $^{****}p = 3.3 \times 10^{-5}$; n.s., $p = 0.73$; For pEC_{50} plot: $^{****}p = 5.4 \times 10^{-6}$, $^{*}p = 0.026$; unpaired, two-tailed t-test. **g**, **h** Molecular docking poses of (**g**) VU0155041 and (**h**) PHCCC in the allosteric pocket within the mGlu$_4$ 7TM domain. **i**, **k** L-AP4-concentration- response curves for mGlu$_{4/4}$ homodimers bearing the indicated mutations near the top pocket (red shaded region in cartoon) (left plots) or near the bottom pocket (blue shaded region in cartoon) (right plots) in the presence or absence of (**i**) VU0155041 (top binding PAM indicated by red region in TM domain of cartoon) or (**k**) PHCCC (bottom binding PAM indicated by blue region in TM domain of cartoon). **j**, **l** The same experimental design as described for (**i**) and (**k**) but for mGlu$_{2/4}$ heterodimers. In all plots, symbols represent the mean drug-induced BRET response and error bars represent ± SEM, and the exact number of '*n*' independent experiments and technical replicates are reported in Supplementary Table 1. Source data are provided as a Source Data file.

earlier findings and show that only a subset of mGlu$_4$ allosteric compounds can mediate positive allosteric effects in mGlu$_{2/4}$ heteromers.

Binding site dependence of mGlu$_4$-selective PAMs

We next turned to investigating the molecular mechanisms and determinants that might explain this differential PAM activity at mGlu$_{4/4}$ homodimers and mGlu$_{2/4}$ heterodimers, the nature of which has remained a complete mystery. A prior study, focused only on mGlu$_{4/4}$ homodimers, used a combination of mutagenesis and molecular docking studies to show the existence of two overlapping binding pockets in the 7TM domain of this receptor for accommodating PAMs. VU0155041 was inferred to bind to the upper-most pocket, referred to as a shallow pocket, whereas PHCCC binds in a second deeper pocket[30]. Thus, we sought to understand whether the subsets of PAMs that bind in these two pockets might also differ in their action in mGlu$_{4/4}$ homodimers compared to mGlu$_{2/4}$ heterodimers.

In contrast to the earlier docking study, which used homology models of the 7TM domain of mGlu$_4$ based on crystal structures of dopamine D3 and mGlu$_1$ receptors, we used the recent cryo-EM

structure of the human $mGlu_{4/4}$ homodimer-G_i complex[31] for an induced-fit molecular docking strategy to investigate PAM binding within the allosteric binding pocket of the $mGlu_4$ 7TM domain. We confirmed the presence of two overlapping sub-pockets for PAMs within the 7TM helical bundle (Fig. 1g, h and Supplementary Fig. 3a, b). VU0155041 and Lu AF21934 bind to an upper sub pocket near the extracellular region within the 7TM domain (Fig. 1g and Supplementary Fig. 3a), whereas PHCCC, VU0418506, ADX88178, and VU0364770 bind in a deeper region within the 7TM domain in a lower pocket (Fig. 1h and Supplementary Fig. 3b). Quantification of specific interactions between the 7TM bundle and the PAMs identified three main groups of interactions established by the ligands in the two different sub-pockets (Supplementary Fig. 3c). These groups comprise residues 1) specific to the PAMs that bind to the top pocket, 2) residues that are shared between the two sub-pockets in the overlapping region, and 3) residues specific to the PAMs that bind in the bottom pocket, the latter of which also includes additional residues deeper within the bottom pocket mainly specific to ADX88178.

To validate our docking results, we examined the effect of mutating $mGlu_4$ residues in the three different groups outlined above on the activation of defined $mGlu_{4/4}$ homomers by different PAMs. We note that the sequence homology between rat $mGlu_4$ and $mGlu_2$ protomers used in our assays and those of human is ~97%, and is 100% within the allosteric pocket of $mGlu_4$. Consistent with VU0155041 and Lu AF21934 interacting predominantly in the upper pocket, $R655^{3.28}Q$ (superscripted generic residue numbers are assigned based on Ballesteros/Weinstein nomenclature[32]) eliminated the PAM activity of both VU0155041 and Lu AF21934 in $mGlu_{4/4}$ homomers in our CODA-RET assay (Fig. 1i, left plot, and Supplementary Fig. 3d). In contrast, this mutation had little to no effect on the PAM activity of PHCCC (Fig. 1k, left plot), VU0418506, VU0364770 or ADX88178 (Supplementary Fig. 3e–g). $W798^{6.48}A$ diminished the PAM activity of VU0155041 (Fig. 1i, right plot) and Lu AF21934 (Supplementary Fig. 3d), but abolished the PAM effects of PHCCC (Fig. 1k, right plot), VU0418506, VU0364770, and ADX88178 (Supplementary Fig. 3e–g), consistent with the docking data showing that W798 participates in both pockets but interacts more profoundly with the bottom pocket PAMs (Supplementary Fig. 3c). $V826^{7.42}M$ in the bottom pocket had minimal effect on the activity of the top pocket binding PAMs, VU0155041 (Fig. 1i, right plot) or Lu AF21934 (Supplementary Fig. 3d), but completely blocked the PAM effects of PHCCC (Fig. 1k, right plot), VU0418506, VU0364770, and ADX88178 (Supplementary Fig. 3e–g). Taken together, these results confirm our and previous docking predictions that PHCCC and other ligands with a similar activity profile bind within the lower pocket of the 7TM of $mGlu_4$, whereas VU0155041 and Lu AF21934 bind in the upper pocket.

Having confirmed our docking results in $mGlu_{4/4}$ homomers, we performed the same CODA-RET experiments described above using VU0155041 and PHCCC, but in the context of the $mGlu_{2/4}$ heteromer, where the effect of these mutations have not been previously studied. The effects of the mutations on VU0155041's action on $mGlu_{2/4}$ heteromers (Fig. 1j) showed a similar pattern as in $mGlu_{4/4}$ homodimers (Fig. 1i), suggesting that VU0155041 exerts its PAM effects in the heterodimer by also binding to the upper pocket of the $mGlu_4$ protomer. PHCCC had no PAM effect on the mutants in $mGlu_{2/4}$ heterodimers (Fig. 1l), consistent with its lack of activity at the wild-type heterodimer. We also considered the possibility that the bottom pocket $mGlu_4$ PAMs might need to bind both protomers to exert their effects, which could explain the differential pharmacology in the heteromer in which only one $mGlu_4$ PAM can bind. However, CODA-RET experiments using $mGlu_{4/4}$ homomers bearing bottom or top pocket mutations such that only one molecule of PHCCC or VU0155041 can bind to the homodimer still showed PAM effects (Supplementary Fig. 3h, i). Thus, these results overall suggest that, when heterodimerized with $mGlu_2$, the bottom allosteric pocket of the $mGlu_4$ protomer is either incapable of binding PHCCC (or the other bottom pocket PAMs), has a dramatically lower affinity for this compound, or that binding to this site no longer mediates a detectable effect on activation.

To further explore the nature of the binding sites, we focused on another $mGlu_4$ preferring PAM, VU0415374 (Fig. 2a)[33], which was shown previously to dock partially into both the upper and lower pockets of $mGlu_4$[30]. Our docking simulations confirmed that this PAM interacts with both pockets (Fig. 2b), with VU0415374 accessing residues in all three interacting regions described above (Supplementary Fig. 3c). In our CODA-RET assay with $mGlu_{4/4}$ homodimers, VU0415374 showed PAM effects as expected[33] (Fig. 2c). Interestingly, however, this PAM showed no effect at $mGlu_{2/4}$ heterodimers (Fig. 2d), exhibiting a profile like the bottom pocket binding PAMs, even though our docking results showed it also interacts with top pocket residues. We carried out experiments to probe whether the observed PAM effect with VU0155041, a top pocket PAM that enhances $mGlu_{2/4}$ activation, could be blocked in a competition experiment with VU0415374 (Fig. 2e). Indeed, the enhancement in BRET signal observed in L-AP4-activated $mGlu_{2/4}$ heterodimers in the presence of VU0155041 was significantly inhibited by VU0415374 cotreatment, but not by ADX88178 (Fig. 2f), a smaller PAM that has little overlap with VU0155041, as illustrated by the comparison of the binding poses of the two PAMs predicted by docking into our $mGlu_4$ receptor model (Supplementary Fig. 3j). Thus, VU0415374 can clearly bind to the $mGlu_4$ protomer in the context of the $mGlu_{2/4}$ heteromer, but unlike in the $mGlu_{4/4}$ homomer, it has no allosteric effect on activation, pointing to differences in the interprotomer communication in these two complexes and not to a loss of the binding site in the heteromer.

Orthosteric agonists cis-activate $mGlu_{2/4}$ heterodimers

While our findings show that only those PAMs that interact predominantly with the upper pocket residues of the $mGlu_4$ protomer are capable of allosterically modulating $mGlu_{2/4}$ heterodimers, how this binding site is differentially coupled to activation in $mGlu_{4/4}$ homomers and $mGlu_{2/4}$ heteromers is unknown. Previous work has demonstrated that $mGlu_{5/5}$ homodimers are activated by orthosteric agonists in both cis- and trans-activation modes[34], whereby agonist activation of one protomer leads to G protein coupling through the same ligand-activated protomer (cis-activation) as well as the other protomer (trans-activation) within this homodimer. We first used CODA-RET in combination with receptor mutations that control which protomer within a $mGlu_{4/4}$ homodimer can bind orthosteric agonists or G protein to understand how this homodimer is activated. To determine whether orthosteric agonists activate the receptors by a cis-activation mechanism, we introduced established mutations that block binding of orthosteric agonists (T182A in $mGlu_4$)[35,36] and also abolish G protein coupling (F781A in $mGlu_4$)[37,38] in the same defined $mGlu_4$ protomer. The other unmodified protomer is functional in both aspects but thus can only be activated through a cis-activation mechanism, a configuration which we refer to as $mGlu_{4/4}$-cis. Likewise, we also introduced the agonist-blocking mutation in one $mGlu_4$ protomer and the G protein blocking mutation in the other protomer to probe for trans-activation, a configuration referred to as $mGlu_{4/4}$-trans.

Relative to wild-type $mGlu_{4/4}$, both $mGlu_{4/4}$-cis (Fig. 3a) and $mGlu_{4/4}$-trans (Fig. 3b) configurations showed dose-dependent L-AP4 activation in our CODA-RET assay, but with reduced efficacy, confirming $mGlu_{4/4}$ homodimers can also signal in both cis- and trans-activation modes like $mGlu_{5/5}$ receptors. The same experiment was carried out using the endogenous agonist glutamate, which, while less potent than L-AP4[39], yielded similar results (Supplementary Fig. 4a). Notably, all structural studies to date of active mGlu receptor homodimers and heterodimers show that only one G protein is bound in a configuration that precludes binding of a second G protein[40]. Therefore, we infer from the reduced CODA-RET signal that there are two populations of dimers that cannot fully interconvert on the time scale

https://doi.org/10.1038/s41467-024-52822-4

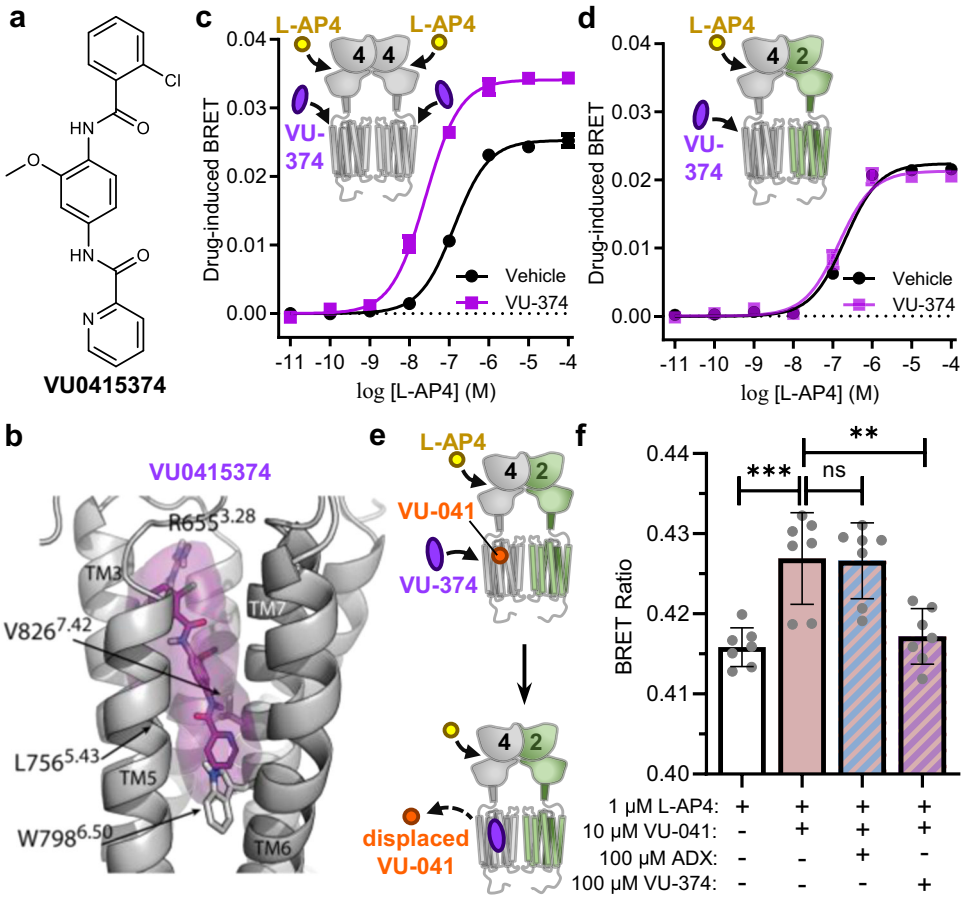

Fig. 2 | The mGlu$_4$ PAM VU0415374 accesses both allosteric binding pockets and binds mGlu$_{2/4}$ heterodimers but is unable to potentiate activity. **a** Structure of VU0415374. **b** Molecular docking pose of VU0415374 in the allosteric binding site(s) within the mGlu$_4$ 7TM domain. **c**, **d** CODA-RET measurements with (**c**) mGlu$_{4/4}$ homodimers or (**d**) mGlu$_{2/4}$ heterodimers showing L-AP4-concentration-response curves in the absence (DMSO vehicle) or presence of 50 μM VU0415374. For the plots in **c** and **d**, symbols represent the mean drug-induced BRET and error bars represent ± SEM. **e** Schematic of PAM competition experiment. **f** PAM competition experiment using CODA-RET with mGlu$_{2/4}$ heterodimers showing the BRET ratio for L-AP4-stimulated receptor in the absence (−) or presence (+) of the indicated PAMs at the concentrations shown. Bars represent the mean BRET ratio, error bars represent ± SD, symbols represent the measured BRET ratio value. For all plots, the exact number of '*n*' independent experiments and technical replicates are reported in Supplementary Table 1. ***$p = 0.0005$; **$p = 0.0024$; n.s., $p = 0.92$, unpaired, two-tailed *t*-test. Source data are provided as a Source Data file.

of our assay, such that a subset can only be activated in either cis- or trans-activation modes; thus, both modes are necessary for full activation of the entire population.

Having established that mGlu$_{4/4}$ homodimers can be both cis- and trans-activated by orthosteric agonists, we next sought to investigate the mechanism of mGlu$_{2/4}$ heterodimer activation. CODA-RET experiments were carried out by expressing heterodimers composed of protomers of unmodified mGlu$_4$ with an mGlu$_2$ protomer bearing the G protein-blocking mutation (F756A in mGlu$_2$)[41] and stimulation with L-AP4 to probe cis-activation via the mGlu$_4$ protomer, a configuration referred to as mGlu$_{2/4}$–4-cis. Likewise, cis-activation mediated by the mGlu$_2$ protomer was tested by expressing heterodimers composed of unmodified mGlu$_2$ with mGlu$_4$ protomers bearing the G protein-blocking mutation stimulated with the mGlu$_2$ agonist DCG IV (Supplementary Fig. 1b), a configuration referred to as mGlu$_{2/4}$–2-cis. Interestingly, in these experiments where the orthosteric agonist is selective for the protomer capable of G protein binding, each receptor showed dose-dependent agonist activation (Fig. 3c, d), indicating that each protomer in the mGlu$_{2/4}$ heterodimer can operate in the cis-configuration. Additionally, these configurations show activation profiles with the selective agonists nearly identical to their wild-type mGlu$_{2/4}$ counterparts, suggesting little to no contribution from the second protomer, whether or not it is capable of G protein binding. Control experiments also confirmed that, at the concentrations used in this study, the orthosteric agonists DCG IV and L-AP4, in the absence or presence of VU0155041 or PHCCC, failed to activate mGlu$_{4/4}$ and mGlu$_{2/2}$, respectively (Supplementary Fig. 4b, c), confirming the reported specificity of these ligands.

To further explore cis-activation in mGlu$_{2/4}$, we expressed heteromers bearing combinations of the mutations that block agonist binding (T168A in mGlu$_2$ or T182A in mGlu$_4$) and/or G protein coupling (F781A in mGlu$_4$ or F756A in mGlu$_2$) in defined protomers and activated the receptors with the nonselective endogenous agonist glutamate (Supplementary Fig. 1b), which has the potential to bind and activate both protomers in wild-type mGlu$_{2/4}$ heteromers. In the mutant receptors used to probe cis-activation, where only one glutamate molecule can bind per dimer, we also observed dose-dependent cis-activation from both protomers in the heterodimer, but with a reduced efficacy relative to wild-type mGlu$_{2/4}$ heteromers (Fig. 3e), providing further evidence that both the mGlu$_4$ and mGlu$_2$ protomers within the wild-type heterodimer contribute to G protein coupling and that activation of both protomers is necessary for full activation. Furthermore, configurations of mutant receptors capable of binding two glutamate molecules per heteromer, but that can only couple to G protein via the mGlu$_2$ or mGlu$_4$ protomer, showed a nearly identical activation profile relative to those mutants that only bind one glutamate molecule per protomer (Supplementary Fig. 4d), again consistent with a lack of signaling by the second protomer when only the

https://doi.org/10.1038/s41467-024-52822-4

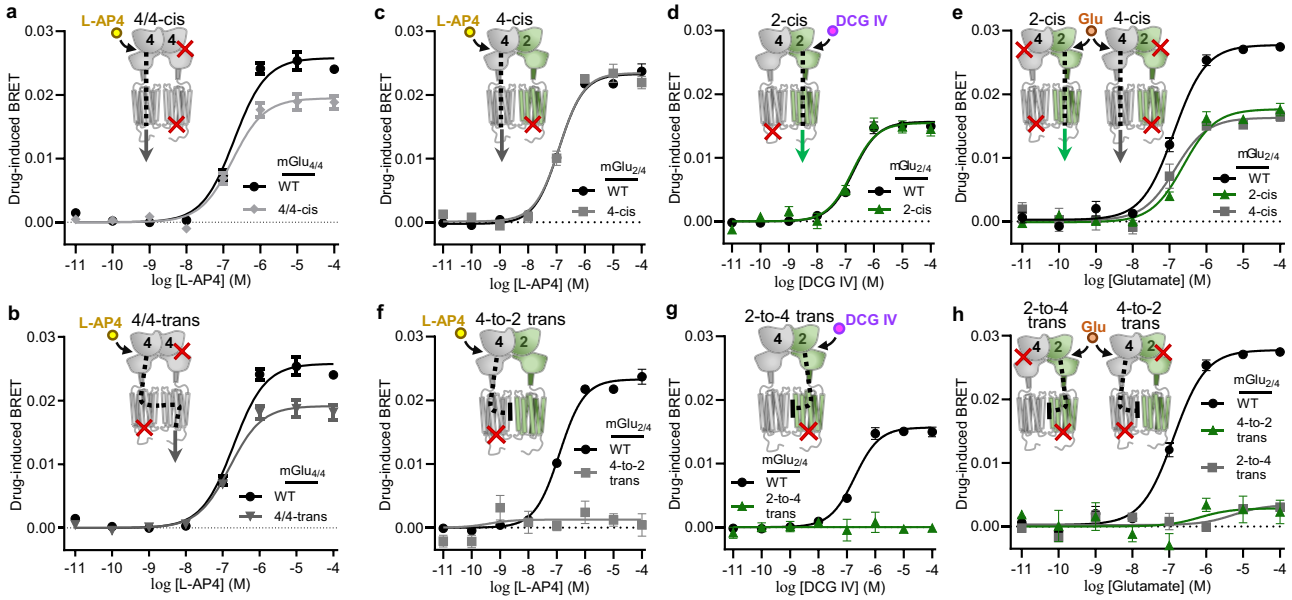

Fig. 3 | Orthosteric agonists efficiently activate $mGlu_{4/4}$ homodimers in both cis and trans mode but only efficiently cis-activate $mGlu_{2/4}$ heterodimers. **a**, **b** CODA-RET measurements showing L-AP4-concentration-response curves for cells expressing (**a**) $mGlu_{4/4}$ homodimers bearing mutations that block orthosteric agonist (denoted by a red X in the VFT domain in schematic) and G protein coupling (denoted by a red X near the bottom of the 7TM domain in schematic) in one protomer to probe for cis-activation by the unmodified protomer (4/4 cis), and (**b**) $mGlu_{4/4}$ homodimers bearing the G protein blocking mutation in one protomer and the agonist-blocking mutation in the other to probe for trans-activation (4/4 trans) compared to wild-type (WT) $mGlu_{4/4}$ homodimers under the same conditions. **c**, **f** CODA-RET measurements showing L-AP4-concentration-response curves for cells expressing $mGlu_{2/4}$ heterodimers bearing G protein-blocking mutations in the indicated protomers (see receptor schematics) to probe for (**c**) cis-activation mediated by the $mGlu_4$ protomer (4-cis) and (**f**) trans-activation mediated by L-AP4 activation of the $mGlu_4$ protomer to the $mGlu_2$ protomer (4-to-2 trans) compared to WT $mGlu_{2/4}$ heterodimers under the same conditions. **d**, **g** The same type of experiments described in **c**, **f**, except the $mGlu_2$ agonist DCG IV is used to stimulate $mGlu_{2/4}$ heteromers with mutations in the indicated protomers to probe for (**d**) cis-activation via the $mGlu_2$ protomer (2-cis) and (**g**) trans-activation mediated by activation of the $mGlu_2$ protomer to the $mGlu_4$ protomer (2-to-4 trans) compared to wild-type $mGlu_{2/4}$ heterodimers under the same conditions. **e**, **h** The same type of experiments described in **c**, **f** and **d**, **g**, except glutamate (Glu) is used to stimulate $mGlu_{2/4}$ heterodimers with mutations in the indicated protomers used to probe for (**e**) 2- or 4-cis activation and (**h**) 2-to-4 or 4-to-2 trans activation compared to WT heteromers under the same conditions. For all plots, symbols represent the mean drug-induced BRET, error bars represent ± SEM, and the exact number of '*n*' independent experiments and technical replicates are reported in Supplementary Table 1. Source data are provided as a Source Data file.

first protomer is activated. We also carried out experiments with wild-type heteromers in which we stimulated with L-AP4 or DCG IV alone compared to when the receptors were stimulated with both agonists, and, in these experiments, we observed a higher E_{max} when both protomers were stimulated relative to when only one protomer of the dimer was activated (Supplementary Fig. 4e), again consistent with two populations of receptor heteromers that cannot interconvert on the time scale of our assay, as we observed for the homomers. This result is consistent with previous work in $mGlu_{5/5}$ homomers, which concluded that while two agonists are required for full activation, substantial partial-like activation was observed with a single agonist[42]. Taken together, the results of these different experiments support a cis-activation mechanism for both protomers, which seem to act independently of each other despite being present in a heteromeric complex.

We next turned to delineating whether orthosteric agonists, in addition to cis-activation, can also trans-activate $mGlu_{2/4}$ heteromers. To this end, we carried out experiments using L-AP4 or DCG IV with heterodimer mutants in which these orthosteric agonists are selective for the protomer bearing the G protein-blocking mutations; thus, G protein recruitment can only occur through trans-activation of the other unmodified protomer. Interestingly, unlike for $mGlu_{4/4}$ homomers, neither of these experiments resulted in detectable activation (Fig. 3f, g), suggesting that neither protomer, when stimulated by its specific orthosteric agonist, substantially trans-activates the other in the context of the heterodimer.

To determine whether the heterodimer can be trans-activated by glutamate, we measured activation of heteromer variants where the agonist-blocking mutation is in one protomer and the G protein mutation in the other protomer. The resulting $mGlu_{2/4}$ heteromer mutants should only activate G protein if glutamate binds the orthosteric site of one protomer and trans-activates G protein through the other protomer. These configurations led to minimal activation by glutamate (Fig. 3h), providing further support that trans-activation between protomers is dramatically blunted in $mGlu_{2/4}$ heterodimers compared to that in $mGlu_{4/4}$ homodimers.

Upper pocket $mGlu_4$ PAMs enable trans-activation in $mGlu_{2/4}$ heteromers

Having characterized the mechanism of orthosteric activation in $mGlu_{2/4}$ heteromers, we next turned to understanding the mechanism of action of the top allosteric pocket binding $mGlu_4$ PAM VU0155041 that maintains function in heterodimers. To probe the effects of VU0155041 on cis-activation of $mGlu_{2/4}$ heterodimers, we performed CODA-RET experiments in which we stimulated the mutant receptors that probe the contribution of cis-activation by the $mGlu_4$ protomer with L-AP4 (as in Fig. 3c) in the presence or absence of VU0155041. In this experiment, VU0155041 enhanced L-AP4-induced cis-activation (Fig. 4a). Analogous experiments using receptor mutants to control the site of glutamate binding in the presence of VU0155041 yielded a similar result (Supplementary Fig. 5a). These experiments suggest, not surprisingly, that VU0155041 allosterically enhances cis-activation of the $mGlu_4$ protomer to which it binds.

We also examined the effects of VU0155041 on cis-activation of the $mGlu_2$ protomer with DCG IV. Interestingly, in this experiment, we also observed enhanced activation (Fig. 4b), suggesting that VU0155041 can allosterically enhance cis-activation at the $mGlu_2$ protomer by binding to the $mGlu_4$ protomer, acting as a "trans-PAM".

https://doi.org/10.1038/s41467-024-52822-4

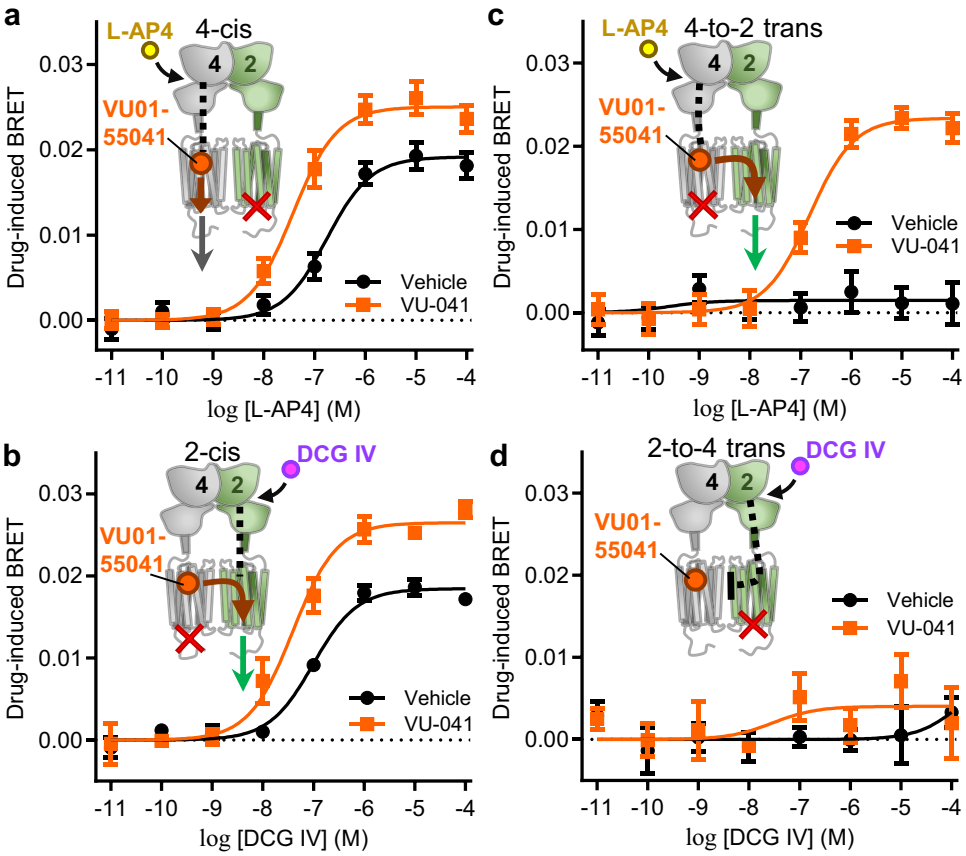

Fig. 4 | VU0155041 enhances cis-activation and enables robust trans-activation in $mGlu_{2/4}$ heteromers. a CODA-RET measurements with $mGlu_{2/4}$ heterodimer mutant described in Fig. 3c legend showing L-AP4-concentration-response curves in the absence (DMSO vehicle) or presence of 50 μM VU0155041. **b** CODA-RET measurements with $mGlu_{2/4}$ heterodimer mutant described in Fig. 3d legend showing DCG IV-concentration-response curves in the absence (DMSO vehicle) or presence of 50 μM VU0155041. **c** CODA-RET measurements with $mGlu_{2/4}$ heterodimer mutant described in Fig. 3f legend showing L-AP4-concentration-response curves in the absence (DMSO vehicle) or presence of 50 μM VU0155041. **d** CODA-RET measurements with $mGlu_{2/4}$ heterodimer mutant described in Fig. 3g legend showing DCG IV-concentration-response curves in the absence (DMSO vehicle) or presence of 50 μM VU0155041. For all plots, symbols represent the mean drug-induced BRET, error bars represent ± SEM, and the exact number of '*n*' independent experiments and technical replicates are reported in Supplementary Table 1. Source data are provided as a Source Data file.

Importantly, this result demonstrates that this PAM can allosterically enable communication from the $mGlu_4$ protomer to the $mGlu_2$ protomer, an effect not apparent in our experiments with orthosteric agonists alone where the protomers seemed to operate in cis-activation mode independently of one another (Fig. 3c, d, f, g). We performed the same experiment in the presence of an $mGlu_4$ NAM, VU0448383 (Supplementary Fig. 5b)[43], which showed NAM effects in both $mGlu_{4/4}$ and $mGlu_{2/4}$ in our CODA-RET experiments (Supplementary Fig. 5c, d), to determine whether negative allosteric modulation of the $mGlu_4$ protomer might have an inhibitory effect on cis-activation of the $mGlu_2$ protomer. Unlike the PAM VU0155041, this particular NAM had no effect on cis-activation of $mGlu_2$ (Supplementary Fig. 5e), suggesting that trans-allosteric communication might only be present with upper pocket PAMs or that a potential trans-NAM effect might also be allosteric pocket specific.

We next sought to test whether VU0155041 binding to the $mGlu_4$ protomer of $mGlu_{2/4}$ heteromers might also enable trans-activation between protomers. As presented earlier, little to no trans-activation is observed in the $mGlu_{2/4}$ mutant when activated by L-AP4 alone (Fig. 3f), an experiment that probes specifically for trans-activation of the $mGlu_2$ protomer. Remarkably, in the presence of VU0155041, we observed robust activation by L-AP4 in the identical configuration (Fig. 4c). This effect was not observed in the same experiment using receptor mutants bearing the G protein-blocking mutation in both protomers (Supplementary Fig. 5f), confirming that this mechanism depends on G protein coupling to the unmodified $mGlu_2$ protomer and ruling out the unlikely possibility that VU0155041 rescues G protein binding to the G protein-blocked $mGlu_4$ protomer. A similar enabling of trans-activation was observed in analogous experiments with $mGlu_{2/4}$ variants selectively activated by glutamate in the presence of VU0155041 (Supplementary Fig. 5g). We also observed trans-activation with the structurally similar PAM Lu AF21934, which also binds in the upper allosteric pocket of the $mGlu_4$ 7TM domain (Supplementary Fig. 5h). Together, these results show that upper allosteric pocket PAMs enable a mechanism by which orthosteric activation of the $mGlu_4$ protomer can allosterically trans-activate the $mGlu_2$ protomer within the heterodimer, allowing interprotomer communication similar to that observed in the $mGlu_{4/4}$ homodimer.

Considering that VU0155041 binding to the $mGlu_4$ protomer can act across the dimer interface to enhance cis-activation of the $mGlu_2$ protomer (Fig. 4b) as well as to enable its trans-activation (Fig. 4c), we sought to determine whether this PAM might also enable trans-activation in the opposite direction upon agonist activation of the $mGlu_2$ protomer. We stimulated the heteromer mutant that probes the contribution of trans-activation of the $mGlu_4$ protomer upon stimulation of the $mGlu_2$ protomer with DCG IV, which we showed earlier does not occur with agonist alone (Fig. 3g). In the presence of VU0155041, we also observed little to no activation in this experiment (Fig. 4d). This result suggests that while VU0155041 can enable efficient trans-activation through allosteric communication from the $mGlu_4$

https://doi.org/10.1038/s41467-024-52822-4

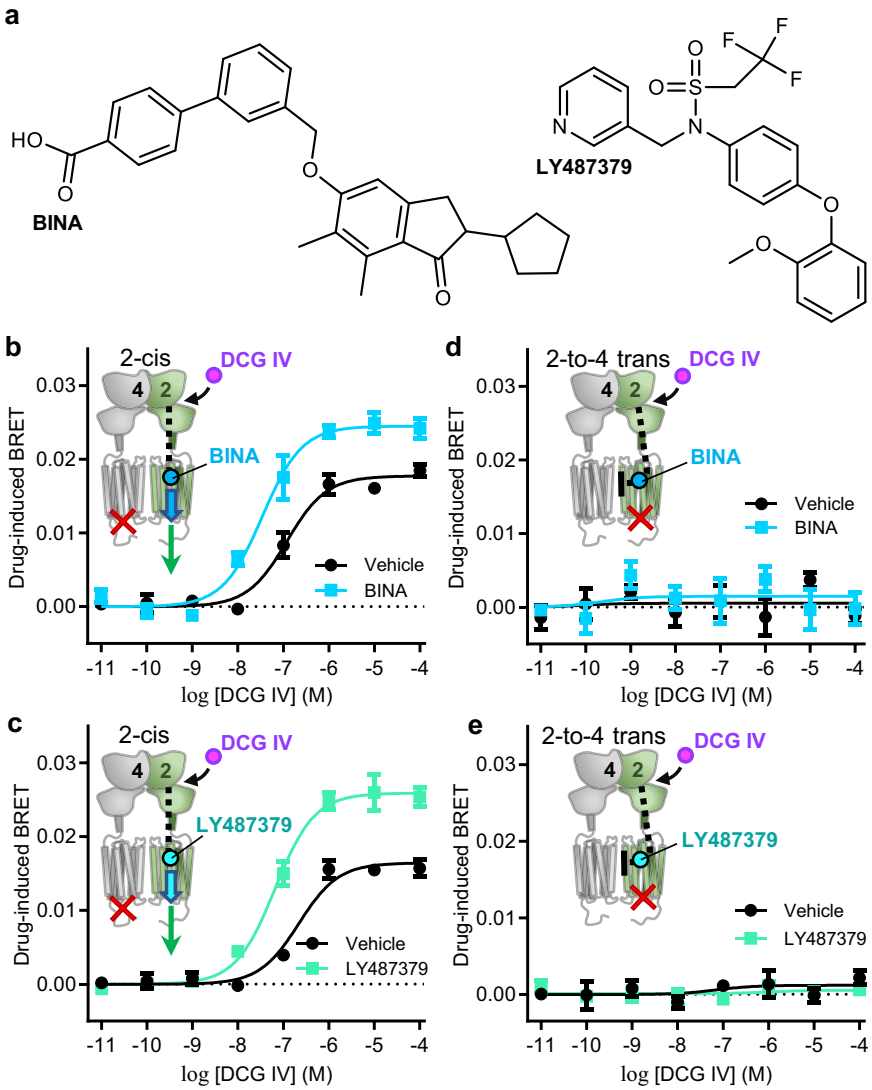

Fig. 5 | Select $mGlu_2$ PAMs mediate their effects on cis-activation of the $mGlu_2$ protomer and have no effect on $mGlu_4$ protomer activation within $mGlu_{2/4}$ heterodimers. a Structures of the $mGlu_2$ PAMs BINA and LY487379. **b**, **c** CODA-RET measurements with the $mGlu_{2/4}$ heterodimer mutant described in Fig. 3d legend showing DCG IV-concentration-response curves in the absence (DMSO vehicle) or presence of 50 μM (**b**) BINA and (**c**) LY487379. **d**, **e** CODA-RET measurements with the $mGlu_{2/4}$ heterodimer mutant described in Fig. 3g legend showing DCG IV-concentration-response curves in the absence (DMSO vehicle) or presence of 50 μM (**d**) BINA and (**e**) LY487379. For all plots, symbols represent the mean drug-induced BRET, error bars represent ± SEM, and the exact number of '*n*' independent experiments and technical replicates are reported in Supplementary Table 1. Source data are provided as a Source Data file.

protomer to the $mGlu_2$ protomer (Fig. 4c), this PAM is unable to facilitate substantial transactivation in the opposite direction from the agonist-stimulated $mGlu_2$ promoter to the $mGlu_4$ protomer.

$mGlu_{2/4}$ heteromer trans-activation is not observed with $mGlu_2$ PAMs

We next turned to exploring the effects of $mGlu_2$ PAMs on $mGlu_{2/4}$ heterodimer activation to determine whether we could detect trans-allosteric communication from the agonist-stimulated $mGlu_2$ promoter to the $mGlu_4$ protomer. We used two structurally distinct and well characterized $mGlu_2$ PAMs, BINA[44], and LY487379[45,46] (Fig. 5a), both of which enhanced activation by the $mGlu_2$ orthosteric agonist DCG IV at $mGlu_{2/4}$ heterodimers in our CODA-RET assay (Supplementary Fig. 6a).

Both BINA and LY487379 enhanced activation of the DCG IV-stimulated heteromer mutants that probe for cis-activation mediated by the $mGlu_2$ protomer (Fig. 5b, c). In contrast, neither BINA nor LY487379 had an effect on heteromer mutants that probe for trans-activation mediated by the $mGlu_2$ protomer to the $mGlu_4$ protomer (Fig. 5d, e). Adding BINA together with VU0155041 also failed to enable trans-activation by DCG IV, as did the addition of PHCCC (Supplementary Fig. 6b, c). Finally, neither BINA nor LY487379 showed effects on L-AP4-activated $mGlu_{2/4}$ heterodimers (Supplementary Fig. 6d, e), suggesting that these PAMs, when bound to the $mGlu_2$ protomers, have little to no trans-PAM effect on $mGlu_4$ protomer activation.

$mGlu_{2/4}$ trans-activation observed in downstream signaling

Our CODA-RET assay measures an increase in the proximity of $G\alpha_i$ to defined mGlu dimers upon agonist activation but not subsequent G protein activation or associated downstream signaling. To provide further evidence of these allosteric mechanisms at the downstream signaling level, we used a BRET-based assay that measures cyclic adenosine monophosphate (cAMP) inhibition[47] mediated by uncomplemented mGlu receptors via $G\alpha_i$ activation upon receptor stimulation in the presence or absence of $mGlu_4$ or $mGlu_2$ PAMs (Fig. 6a).

Consistent with our CODA-RET results, but in the absence of receptor-mediated RLuc8 complementation, both VU0155041 and

https://doi.org/10.1038/s41467-024-52822-4

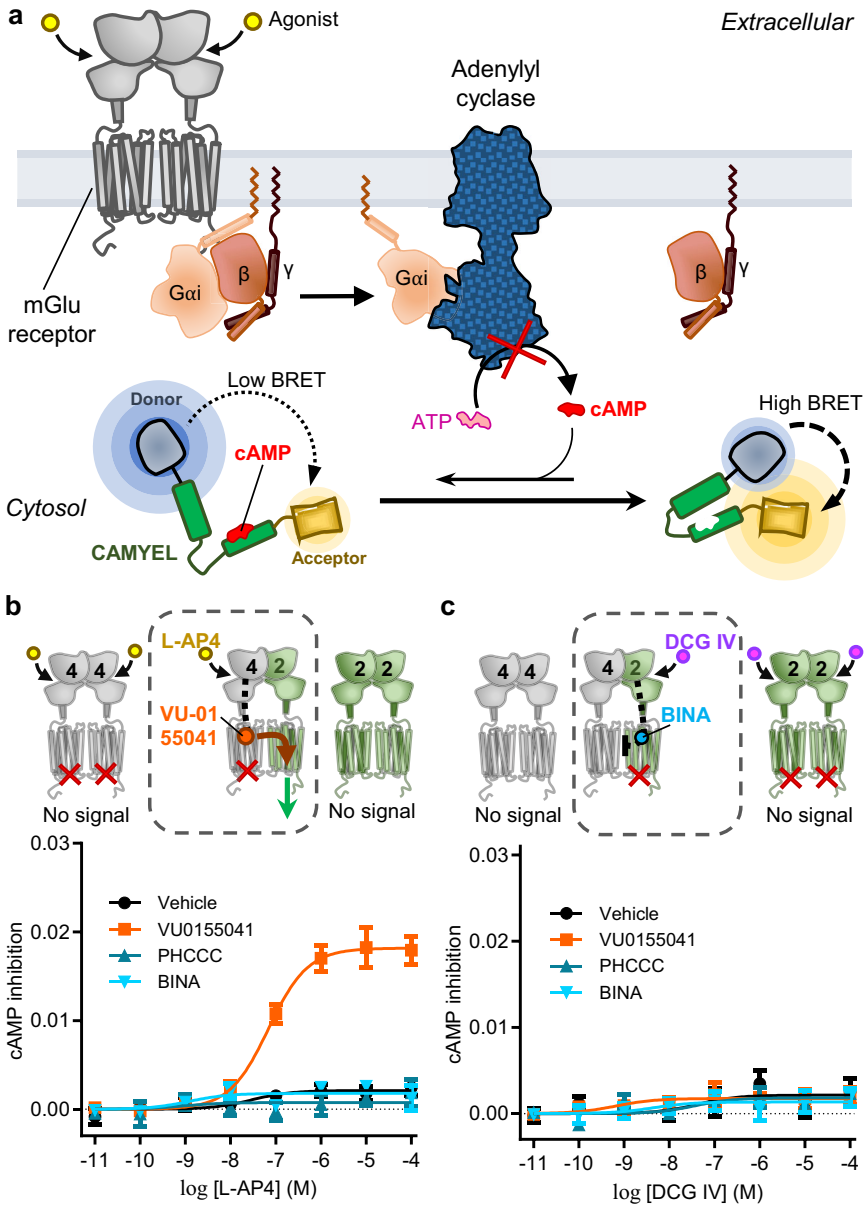

Fig. 6 | $mGlu_{2/4}$ trans-activation observed in cAMP inhibition experiments. **a** Schematic of the BRET-based cAMP inhibition assay. Agonist-activated group II or III mGlu homodimers or heterodimers couple to and activate the heterotrimeric G_i protein leading to inhibition of adenylyl cyclase and decreased cAMP biosynthesis from adenosine triphosphate (ATP). The cAMP sensor using YFP-Epac-RLuc (CAMYEL)[47] was used to detect cAMP inhibition. **b** (top) Schematic showing experiment probing trans-activation from the $mGlu_4$-to-$mGlu_2$ protomer and corresponding cAMP-inhibition measurements showing L-AP4-concentration-response curves in the absence (DMSO vehicle, black circles) or presence of 50 μM PAMs: VU0155041 (orange squares), PHCCC (cyan triangles), BINA (blue inverted triangles). **c** (top) Schematic showing experiment probing trans-activation from the $mGlu_2$-to-$mGlu_4$ protomer and corresponding cAMP-inhibition measurements showing DCG IV-concentration-response curves in the absence (DMSO vehicle, black circles) or presence of 50 μM PAMs: VU0155041 (orange squares), PHCCC (cyan triangles), BINA (blue inverted triangles). For plots, symbols represent the mean drug-induced BRET, error bars represent ± SEM, and the exact number of '*n*' independent experiments and technical replicates are reported in Supplementary Table 1. Source data are provided as a Source Data file.

PHCCC showed PAM effects at $mGlu_{4/4}$ homodimers, as did BINA at $mGlu_{2/2}$ homodimers, showing that the cAMP assay can detect PAM-mediated effects (Supplementary Fig. 7a and 7b). However, because heterodimer signaling cannot be isolated in the cAMP assay in the same manner as CODA-RET, we used a combination of mGlu protomer-specific agonists and the G protein-blocking mutations employed above, but in the absence of complementation, to isolate cAMP effects induced specifically by $mGlu_{2/4}$ heterodimers. Thus, to determine if we could observe a cAMP response from trans-activation of $mGlu_{2/4}$, we co-expressed $mGlu_4$ protomers bearing the G protein-blocking mutation with unmodified $mGlu_2$ protomers and activated the receptors with the $mGlu_4$ agonist L-AP4 (Fig. 6b, top schematic). In this experiment, $mGlu_4$ homodimers with the mutation in both protomers can bind agonist but are unable to couple to $G\alpha_i$ and thus cannot inhibit cAMP production (Supplementary Fig. 7c). Similarly, $mGlu_{2/2}$ homodimers are not activated by L-AP4[48] (Supplementary Fig. 4b) and thus do not mediate cAMP signaling. Therefore, the population of expressed $mGlu_{2/4}$ heterodimers can signal in this context only if the effects of L-AP4 on the $mGlu_4$ protomer are mediated by trans-activation of the $mGlu_2$ protomer (Fig. 6b, top schematic, dashed box).

In concordance with our CODA-RET experiments, we observed no L-AP4-stimulated cAMP inhibition in the absence of PAMs or in the presence of PHCCC (Fig. 6b, bottom plot), providing evidence

that transactivation is not observed at the downstream cAMP level with only orthosteric agonist activation or when a bottom pocket-binding PAM is added. We also observed no effect with the $mGlu_2$ PAM BINA in these experiments, providing further support that allosteric modulation of $mGlu_2$ has no detectable effect on this trans-activation mechanism. However, as predicted by our CODA-RET results (Fig. 4c), we observed robust L-AP4-induced cAMP inhibition in the presence of VU0155041 (Fig. 6b, bottom plot), demonstrating that this PAM enables trans-activation by binding the $mGlu_4$ protomer and enabling L-AP4 to activate G protein through coupling to the $mGlu_2$ protomer. These data demonstrate that the $G\alpha_i$ recruitment to defined $mGlu_{2/4}$ heterodimers observed in our CODA-RET assay is associated with bona fide G protein activation and downstream signaling.

Having applied the cAMP assay to detect trans-activation from the $mGlu_4$ protomer to $mGlu_2$ protomer, we next used the same type of experiment described above to probe cAMP inhibition mediated by trans-activation from the $mGlu_2$ to the $mGlu_4$ protomer. Here, we co-expressed unmodified $mGlu_4$ with $mGlu_2$ protomers bearing the G protein-blocking mutation and activated the receptors with the $mGlu_2$ agonist DCG IV (Fig. 6c, top schematic). In this scenario, $mGlu_{4/4}$ homodimers are not DCG IV-stimulated[49] (Supplementary Fig. 4c) and DCG IV-stimulated $mGlu_{2/2}$ homodimers are unable to couple to $G\alpha_i$ and therefore cannot inhibit cAMP production (Supplementary Fig. 7d). In this experiment, the population of $mGlu_{2/4}$ heterodimers can signal only if the effects of DCG IV on the $mGlu_2$ protomer are allosterically communicated to the $mGlu_4$ protomer (Fig. 6c, top schematic, dashed box). Consistent with our inability in CODA-RET experiments to observe trans-activation in this direction (Fig. 5d), we also failed to detect DCG IV-stimulated cAMP in the absence or presence of the $mGlu_2$ PAM BINA (Fig. 6c, bottom plot) or the $mGlu_4$ PAMs VU0155041 or PHCCC.

Discussion

Our findings that $mGlu_4$-targeted PAMs have differential activity in vitro and in vivo led us to hypothesize that this behavior could be explained by their differential pharmacology at $mGlu_{4/4}$ homomers and $mGlu_{2/4}$ heteromers. In particular, whereas VU0155041 and Lu AF21934 have been effective in every brain circuit tested, PHCCC and VU0418506 are inactive at corticostriatal[18,22] and thalamocortical[19] synapses, consistent with our hypothesis that the effects of group III agonists at these synapses are mediated predominantly by an $mGlu_4$ containing heteromer. Most likely these effects are mediated by $mGlu_{2/4}$ heteromers based on the ability of MRK-8-29, a $mGlu_2$ selective NAM, to inhibit L-AP4-induced effects on thalamocortical synaptic transmission[19]. Here, using our in vitro CODA-RET assay, we confirmed that VU0155041 and Lu AF21934 are active at $mGlu_{2/4}$ heteromers, whereas PHCCC, VU0418506, and a number of additional compounds, are inactive at these heteromers despite their robust activity at $mGlu_{4/4}$ homomers. Consistent with these results, a nanobody approach for detecting endogenous levels of these receptors in the brain has supported the presence of $mGlu_{2/4}$ heterodimers in the striatum and prefrontal cortex[15].

Using the $mGlu_{4/4}$ cryo-EM structure for virtual docking studies, we confirmed the existence of two overlapping allosteric pockets in the 7TM domain. VU0155041 and Lu AF21934 bind to the upper allosteric pocket, whereas PHCCC, VU0418506, VU0364770, and ADX88178 bind to a lower pocket deeper into the 7TM domain. Our work is consistent with a prior study that also demonstrated that VU0155041 binds an upper pocket in $mGlu_{4/4}$ homodimers whereas PHCCC and several other PAMs bind a lower pocket[30]. The lack of effect of the bottom pocket PAM ADX88178 on the activity of the top pocket ligand VU0155041 in our competition experiment using the CODA-RET assay in $mGlu_{2/4}$ heteromers is consistent with their ability to bind simultaneously. It is also possible, however, that the bottom pocket is not accessible for binding PAMs in the $mGlu_{2/4}$ heteromer, reminiscent of the finding that the allosteric site for PAMs in $mGlu_{2/2}$ is not formed in the inactive protomer in the active $mGlu_{2/2}$ homomer structure[41]. Curiously, in the recent $mGlu_{2/4}$ heteromer structure[50], Met663, Tyr667, and Leu670 from TM3 are rotated into the binding site such that they could sterically occlude binding to the bottom pocket of the $mGlu_4$ protomer (Supplementary Fig. 8a and 8b). However, a revised analysis of the $mGlu_{4/4}$ homomer structure[50] highlighted uncertainty in the position of these side chains, making it difficult to reach a conclusion on the accessibility of this site in the homomer. Regardless, VU0415374, a compound that binds in the middle of the overlapping allosteric pockets, still binds the $mGlu_{2/4}$ heteromer, based on its ability to compete with VU0155041, but is nonetheless inactive from the perspective of PAM activity. The bottom pocket might also be able to accommodate the ligands in the heteromer without effect, thereby acting as neutral allosteric compounds in the context of the heteromer, or these compounds might bind but with substantially lower affinity than to the homomer.

The mGlu homomer and heteromer structures to date have only revealed PAM binding to the G protein-coupled protomer, referred to as the active protomer. The ability of the upper pocket $mGlu_4$ PAMs to enhance cis-activation via DCG IV-stimulation of the $mGlu_2$ protomer in $mGlu_{2/4}$ heteromers demonstrates that PAMs can also bind the protomer not coupled to G protein, the inactive $mGlu_4$ protomer, producing a conformational change that acts as a trans-PAM across the interprotomer interface to enhance activation and G protein coupling of the active protomer. Thus, while there is substantial evidence for asymmetric activation of mGlu receptors[40,50–52], our results suggest that the activation mechanism is more complex, and that we must independently consider orthosteric agonist-, allosteric modulator-, and G protein-binding to both protomers, which interact in complex patterns that may differ across different heterodimer pairs. In the scenario of a trans-PAM, the protomer not bound to G protein must assume a PAM-induced, active-like configuration that is transmitted to the active protomer that couples to G protein. Thus, when bound to a trans-PAM, the protomer not coupled to G protein can no longer be considered inactive. Additional structures and biophysical experiments will be necessary to deduce the atomic-level details of these conformational changes, but the molecular logic can be defined by the types of experiments we have developed here. Notably, in the calcium sensing receptor, another dimeric class C receptor, PAMs can bind both protomers of an active complex[53–55], confirming the structural feasibility of our mechanistic findings.

Here we show that $mGlu_{4/4}$ homodimers can be both cis- and trans-activated by orthosteric ligands, whereas the individual protomers in $mGlu_{2/4}$ can only be cis-activated by these ligands. The upper pocket PAMs enable trans-activation in the heteromer, presumably by altering the interprotomer interface in a manner that the bottom or middle pocket PAMs cannot. The recent $mGlu_{2/4}$ structure gives no clear clues as to the nature of these different interactions, as the interprotomer interfaces in the homomer and heteromer structures are quite similar, although we do note a small change in the relative orientation of the protomers that might impact interprotomer communication (Supplementary Fig. 8c)[50]. Indeed, while the structures to date of class C receptors show a transition to a TM6-TM6 interprotomer interface upon activation, the details and packing of these interfaces differ somewhat across receptors[51], allowing for a diversity of heterodimer interfaces that could be further altered by the binding of PAMs and NAMs. Thus, more work will be required to capture the structural basis of differential trans-allostery.

We note that our findings differ in several aspects from two prior studies of the activation mechanism of $mGlu_{2/4}$ heteromers[50,56]. Both of these studies reported trans-activation from the $mGlu_2$ to $mGlu_4$ protomer. In contrast, we did not observe this in any of our experiments with or without the PAMs explored here. There are many methodological differences that make it difficult to ascertain the

reason for the discrepancies. First, these studies used the gamma-aminobutyric B ($GABA_B$) receptor C-tail retention system to control heteromeric assembly and surface expression, and this involves partial truncation of the mGlu native C tails. This truncation and/or the addition of the $GABA_B$ receptor tails may alter the heteromer interface of the receptor population that are transported to the surface. Indeed, structural biology approaches have shown that the C tail of the $mGlu_2$ receptor is important for G protein activation[41], and these truncations might impact G protein coupling. In contrast, our CODA-RET approach applies no such control over expression and uses full-length receptor protomers, which we believe serves as a more native-like system to study these complexes and their pharmacology. Liu et al.[56] also employed an artificial chimeric G protein based on $G\alpha_q$ so that assays for calcium flux and inositol monophosphate accumulation could be employed for detection of mGlu receptor activation, rather than the $G\alpha_i$ protein that we used in our CODA-RET assay and that natively couples to $mGlu_2$ and $mGlu_4$. It is possible that the chimera may couple differently to these receptors compared to the native G_i protein.

In one of these studies, Wang et al. also reported a cryo-EM structure of the active $mGlu_{2/4}$ heteromer, expressed and purified in the absence of the $GABA_B$ C tail retention system, in which the G_i protein was in fact bound to the $mGlu_2$ protomer[50], in contradiction with their own cell signaling data and with that reported in the other prior study[56], both of which used the $GABA_B$ tail system for signaling assays. This structure clearly establishes that G_i can bind to $mGlu_2$ in the heteromer, as we show in our CODA-RET assays. Our findings at the level of cAMP signaling in the absence of any complementation are fully consistent with our CODA-RET results and our proposed mechanism, and therefore argues against a confound in the CODA-RET experiments related to the complementation system.

In another prior study, Kammermeier investigated the pharmacologic profile of $mGlu_2$ and $mGlu_4$ protomers when co-expressed recombinantly in isolated rat superior cervical ganglion neurons, which were reported to provide a null-mGlu receptor background[21]. Using patch-clamp recorded inhibition of calcium currents, this study found that activation of a presumed $mGlu_{2/4}$ heterodimer was not evident in the presence of the selective orthosteric agonist, L-AP4 or DCG IV, when applied alone, but apparent activation of the presumed heterodimer was observed when both of these agonists were applied together. Based on these data, this study concluded that $mGlu_{2/4}$ heterodimers require binding of orthosteric agonist to both protomers for activation, which is in conflict with our study, as well as with two prior reports[17,18], that show that one agonist is sufficient to activate the heterodimer. It is difficult to determine what is responsible for these differences in findings, but we speculate that this may be related to the receptor populations that are expressed and that are signaling in these experiments, which are likely a combination of homomers and heteromers, although we cannot rule out a role of the different cellular context as well.

While we have focused here on the impact of PAMs on heteromer activation, the effect of NAMs is quite intriguing as well. In the presence of an upper pocket PAM, we observe an inherent asymmetry, with $mGlu_4$ enabling trans-activation of $mGlu_2$ as well as enhancing cis-activation of the $mGlu_2$ protomer through a trans-PAM effect. In contrast, we detect no such parallel effects from $mGlu_2$ to $mGlu_4$ using these PAMs. Nonetheless, there is still clearly an element of allosteric communication in this direction as $mGlu_2$ (MRK-8-29) or $mGlu_{2/3}$ (MNI-137) NAMs are able to act at $mGlu_2$ as trans-NAMs to inhibit $mGlu_4$ cis-activation[18,19]. In contrast, we show here that the $mGlu_4$ NAM VU0448383 has no trans-NAM effect in $mGlu_{2/4}$ heteromers, again implying that the communication is asymmetric, although we cannot rule out the possibility that $mGlu_2$ PAMs or $mGlu_4$ NAMs that potentially bind in different allosteric pockets might show activity in the heteromer.

Taken together, we have uncovered a fascinating complexity of class C GPCR function that will require careful analysis of the molecular logic for each mGlu heteromer pair. While the existence of the different allosteric pockets may simply be a fortuitous accident of molecular structure that provides pharmacologists an exciting approach to precision control of neural circuits, it is also conceivable that nature has already taken advantage of these pockets through endogenous allosteric modulators. While no such endogenous allosteric modulators of mGlu receptors have yet been identified, we note that endogenous lipids bind within the TM domains of the $GABA_B$ heterodimer, another representative class C receptor. While these lipids have been implicated in structural stability and limiting constitutive activity of this heteromer[57,58], they conceivably might also play a role analogous to the top pocket $mGlu_4$ PAMs by also allosterically enabling trans-activation of the $GABA_{BR2}$ protomer by agonist binding to $GABA_{BR1}$.

Finally, all small molecule allosteric modulators identified to date that target mGlu receptors, by definition, target homodimers, as this is how they were screened. Thus, while we have been able to show that a subset of $mGlu_{4/4}$-targeted PAMs also can target $mGlu_{2/4}$ heteromers, other PAMs cannot. What would be more promising from a precision pharmacology perspective would be the discovery of small molecule allosteric modulators that selectively target defined mGlu heteromers, without engaging homomers or other heteromers containing the targeted protomer. The work presented here provides insights into the molecular logic underlying heterodimer activation and allosteric modulation that are critical to the development and validation of new compounds that target specific mGlu receptor populations in the brain, which could result in precision targeted therapies for a variety of central nervous system disorders. By employing CODA-RET or screening assays using the combination of targeted mutations outlined herein, it will now be possible to identify such compounds. This logic and approach can be extended as well to the many other mGlu or class C receptor heteromers that have been reported[20,59,60] as well as to other dimeric GPCRs[40,61,62] where different homo- and heteromeric assembly of protomers might influence their function and pharmacology.

Methods

Reagents and Ligands

L-AP4, DCG IV, VU0155041, Lu AF21934, PHCCC, VU0364770, BINA and LY487379 were purchased from Tocris Bioscience. 10 mM stock solutions of L-AP4 and DCG-IV were prepared in Dulbecco's phosphate buffered saline (DPBS). 100 mM L-glutamate stock solutions were prepared by dissolving L-glutamic acid (Sigma-Aldrich) in 1 M NaOH. The preparation of VU0418506[63], ADX88178[64], VU0415374[33] and VU0448483[43] compounds were described previously. 10 mM stock solutions of all PAMs and NAMs used in this study were prepared in dimethyl sulfoxide (DMSO). Polyethylenimine (PEI) was purchased from Polysciences Inc. and dissolved in sterile water at 1 mg/ml stock concentration. Coelenterazine H was purchased from Dalton Pharma Services and dissolved in absolute ethanol at 5 mM concentration.

Plasmids

The pcDNA3.1 (+) expression plasmids coding for wild-type rat $mGlu_4$ and $mGlu_2$ protomers tagged at their C-terminus with the RLuc8 fragments L1 (residues 1-229) and/or L2 (residues 230-311), respectively, were described previously[16,19]. All of the indicated point mutations in $mGlu_4$ were prepared in the expression plasmids above using QuikChange site-directed mutagenesis per manufactures protocol (Agilent). The pcDNA3.1 (+) expression plasmids coding for $G\alpha_i$ with mVenus inserted at position 91, untagged $G\beta_1$, and untagged $G\gamma_2$ were described previously[16,19]. The plasmid encoding the cAMP sensor using YFP-Epac-RLuc (CAMYEL) was described previously[47]. All plasmids

generated and used in this study were confirmed by DNA sequencing (Psomagen).

Cell culture and transfections

All cell-based assays were carried out in 293 T cells (ATCC, CRL-3216) from embryonic kidney tissue of *Homo sapiens* (HEK293T). The cells are female in origin and were authenticated by the manufacture using short tandem repeat analysis to determine species and unique DNA profile. The cells were maintained in Dulbecco's modified Eagle's medium (DMEM), high glucose (Gibco) supplemented with 10% fetal bovine serum (Corning Inc.) and 1% penicillin-streptomycin (Corning Inc.) at 37 °C with 5% CO_2. Prior to transfection, HEK293T were grown to ~70% confluency in 10 cm tissue culture dishes. The HEK293T cells used in this study tested negative for mycoplasma contamination.

For the CODA-RET assays, the pcDNA 3.1 (+) plasmids encoding wild type and/or mutant $mGlu_4$ or $mGlu_2$ protomers ($mGlu_4$ homodimer expression: 8 μg $mGlu_4$-L1 and 8 μg $mGlu_4$-L2; $mGlu_2$ homodimer expression: 4 μg $mGlu_2$-L1 and 4 μg $mGlu_2$-L2; $mGlu_{2/4}$ heterodimer expression: 8 μg $mGlu_4$-L1 and 4 μg $mGlu_2$-L2) were co-transfected with 2 μg $G\alpha_i$ tagged with mVenus and 1 μg untagged $G\beta_1$ and 1 μg untagged $G\gamma_2$ into HEK293T cells using PEI at a ratio of 2 μg PEI per 1 μg total plasmid. Transfected cells were incubated at 37 °C with 5% CO_2 for 48 h. Note that prior to experiments, the cells were incubated with DMEM, high glucose, GlutaMAX supplement, pyruvate (Gibco) in the absence of fetal bovine serum for 1 h at 37 °C with 5% CO_2.

For the cAMP assay, the pcDNA 3.1 (+) plasmids encoding wild type and/or mutant $mGlu_4$ or $mGlu_2$ protomers ($mGlu_4$ homodimer expression: 8 μg $mGlu_4$-L1; $mGlu_2$ homodimer expression: 4 μg $mGlu_2$-L1; $mGlu_{2/4}$ heterodimer expression: 8 μg $mGlu_4$-L1 and 4 μg $mGlu_2$-L1), which cannot complement to produce functional RLuc8, were co-transfected with 6 μg of the CAMYEL plasmid into HEK293T cells using PEI at a ratio of 2 μg PEI per 1 μg total plasmid. The same expression protocol described for the CODA-RET assay was followed for the cAMP assay.

CODA-RET assay

After expression, the cells were dissociated from the 10 cm plate using enzyme-free dissociation solution (Millipore-Sigma). After dissociation, the cells were collected and spun at 1000 g for 5 min. The supernatant was discarded, and the cells were washed twice with pre-warmed DPBS. Approximately 300,000 cells per well were distributed in black frame, white well 96-well plates (PerkinElmer) and stimulated with the indicated ligands dissolved in pre-warmed DPBS for 5 min at 37 °C. 5 μM coelenterazine H, the substrate for RLuc8, was added to each well and immediately after the addition of coelenterazine H, DPBS containing the indicated mGlu receptor agonist and PAM or vehicle was loaded to each well. For the competition assay, after expression the cells were pre-incubated with DPBS containing 10 μM VU0155041 for 5 min after dissociating and washing. The cells were distributed in a 96-well plate for the assay as described above. 5 μM coelenterazine H was loaded to each well, then DPBS containing the indicated mGlu receptor agonist and PAMs was loaded into each well immediately. Five min after ligand stimulation, the fluorescence and luminescence signals were quantified using a Pherastar FS plate reader (BMG Labtech). The BRET ratio was determined by calculating the ratio of mVenus signal (525 nm) divided by the RLuc8 (485 nm) signal. The results are expressed as the BRET change produced by the corresponding ligands.

cAMP assay

The cells were dissociated, washed, and plated as described above for the CODA-RET assay. Approximately 60,000 cells per well were distributed in 96-well plates and stimulated by indicated ligands dissolved in pre-warmed DPBS containing 10 μM forskolin for 30 min at 37 °C. 5 μM coelenterazine H was added to each well 5 min before reading. The fluorescence and luminescence were quantified and data analyzed as described above.

Plotting and statistics

Data from the CODA-RET and other BRET-based live cell assays were plotted and fit using GraphPad Prism (GraphPad Software). The dose-response curves of agonist and PAM responses were fitted by non-linear regression to the log(agonist) vs. response model with a standard Hill slope equal to 1 and the bottom fit constrained to 0. To determine p values, an unpaired, two-sided t-test was used, where comparison with $p > 0.05$ were considered statistically significant. Statistical details of experiments can be found in the figure legends. The exact number of 'n' independent experiments and technical replicates are reported in Supplementary Table 1. The E_{max} and pEC_{50} distributions determined from select dose-response curves and statistical comparisons are shown in Supplementary Fig. 9. The baseline luminescence signals from the complemented RLuc8 for each mGlu homomer and heteromer combination tested in our CODA-RET assay are similar in magnitude and shown in Supplementary Fig. 10.

Receptor model

A model of the transmembrane domain of the $mGlu_4$ receptor was obtained from chain R of the cryo-EM structure of the G_i-bound receptor (PDB: 7E9H)[31], including residues from L581 to H848 at the cytoplasmic end of TM7. The model was refined and prepared for docking with the Prime software in the Schrödinger Small-Molecule Drug Discovery Suite (Release 2021-4).

Binding pocket recognition

We employed the SiteMap algorithm to analyze the transmembrane region of the prepared model as well as chain 4 of the $mGlu_4$ cryo-EM structure in complex with the G_i-bound $mGlu_2$ (PDB: 8JD5)[50], prepared using the same protocol described above.

We set a minimum requirement of at least 15 points per reported site, using a standard grid with the default restrictive definition of hydrophobicity. Site maps were cropped at 4 Å from the nearest site point. During the analysis, any pockets identified in the intercellular region or located on the outside of the transmembrane domain were discarded from further consideration to focus solely on relevant findings within the helical bundle.

Docking

Three-dimensional models of all ligands were prepared using the Schrödinger LigPrep ligand preparation protocol. The chirality of the active stereoisomer of VU0155041 was selected as (1 R,2S), according to reported experimental activity[65]. Chirality of Lu AF21934 was determined as (1 R,2S) as well, by analogy with VU0155041. The (−)-PHCCC stereoisomer was used for PHCCC[29]. Protonation states were determined by selecting the most populated species at pH 7.0 according to a semi-empirical model. The Glide Induced Fit docking protocol was used to dock all ligands to a representative conformation of the most populated cluster identified by the trajectory clustering. The center of the docking box was determined by the center of mass of the residues $M663^{3.40}$ and $W798^{6.50}$. In the refinement step, residues within 5.0 Å of the ligands were included in the minimization, and the extra-precision protocol was used for the docking. The best scoring pose was selected for all ligands. Docking was executed using the Glide program in the Schrödinger Small-Molecule Drug Discovery Suite, Release 2019-1.

Clustering

Interaction fingerprints were calculated by identifying residues establishing interactions with the ligand. H-bond interactions were considered formed if the distance between the hydrogen and the

acceptor heavy atom were <2.5, and the angle between the donor, hydrogen, and acceptor was more than 120°. Other interactions were considered formed with a distance cut-off of 4 Å between heavy atoms. To group the ligands based on the similarity of their binding poses, ligand interaction fingerprints were clustered using hierarchical agglomerative clustering with average linkage. Similarly, to identify groups of interactions simultaneously involved in the binding, the residue interaction fingerprints were clustered using the same algorithm.

Reporting summary

Further information on research design is available in the Nature Portfolio Reporting Summary linked to this article.

Data availability

The source data generated in this study are provided in the Source Data file. All Software used to collect and analyze data for this work was either published previously or is commercially available. Source data are provided with this paper.

References

1. Niswender, C. M. & Conn, P. J. Metabotropic glutamate receptors: physiology, pharmacology, and disease. *Annu. Rev. Pharmacol. Toxicol.* **50**, 295–322 (2010).
2. Srivastava, A., Das, B., Yao, A. Y. & Yan, R. Metabotropic glutamate receptors in alzheimer's disease synaptic dysfunction: therapeutic opportunities and hope for the future. *J. Alzheimers Dis.* **78**, 1345–1361 (2020).
3. Masilamoni, G. J. & Smith, Y. Metabotropic glutamate receptors: targets for neuroprotective therapies in Parkinson disease. *Curr. Opin. Pharmacol.* **38**, 72–80 (2018).
4. Conn, P. J., Battaglia, G., Marino, M. J. & Nicoletti, F. Metabotropic glutamate receptors in the basal ganglia motor circuit. *Nat. Rev. Neurosci.* **6**, 787–798 (2005).
5. Dogra, S. & Conn, P. J. Targeting metabotropic glutamate receptors for the treatment of depression and other stress-related disorders. *Neuropharmacology* **196**, 108687 (2021).
6. Peterlik, D., Flor, P. J. & Uschold-Schmidt, N. The emerging role of metabotropic glutamate receptors in the pathophysiology of chronic stress-related disorders. *Curr. Neuropharmacol.* **14**, 514–539 (2016).
7. Dogra, S. & Conn, P. J. Metabotropic glutamate receptors as emerging targets for the treatment of schizophrenia. *Mol. Pharmacol.* **101**, 275–285 (2022).
8. Mazzitelli, M. & Neugebauer, V. mGlu3 metabotropic glutamate receptors-new hope for pharmacotherapy of schizophrenia. *Biol. Psychiatry* **90**, 356–358 (2021).
9. Conn, P. J. & Pin, J. P. Pharmacology and functions of metabotropic glutamate receptors. *Annu. Rev. Pharmacol. Toxicol.* **37**, 205–237 (1997).
10. Romano, C., Yang, W. L. & O'Malley, K. L. Metabotropic glutamate receptor 5 is a disulfide-linked dimer. *J. Biol. Chem.* **271**, 28612–28616 (1996).
11. Asher, W. B. et al. Single-molecule FRET imaging of GPCR dimers in living cells. *Nat. Methods* **18**, 397–405 (2021).
12. Pin, J.-P. & Acher, F. The metabotropic glutamate receptors: structure, activation mechanism and pharmacology. *Curr. Drug Targets. CNS Neurol. Disord.* **1**, 297–317 (2002).
13. Doumazane, E. et al. A new approach to analyze cell surface protein complexes reveals specific heterodimeric metabotropic glutamate receptors. *FASEB J* **25**, 66–77 (2011).
14. Lee, J. et al. Defining the homo- and heterodimerization propensities of metabotropic glutamate receptors. *Cell Rep.* **31**, 107605 (2020).
15. Meng, J. et al. Nanobody-based sensors reveal a high proportion of mGlu heterodimers in the brain. *Nat. Chem. Biol.* **18**, 894–903 (2022).
16. Niswender, C. M. et al. Development and antiparkinsonian activity of VU0418506, a selective positive allosteric modulator of metabotropic glutamate receptor 4 homomers without activity at mGlu2/4 heteromers. *ACS Chem. Neurosci.* **7**, 1201–1211 (2016).
17. Moreno Delgado, D. et al. Pharmacological evidence for a metabotropic glutamate receptor heterodimer in neuronal cells. *Elife* **6**, e25233 (2017).
18. Yin, S. et al. Selective actions of novel allosteric modulators reveal functional heteromers of metabotropic glutamate receptors in the CNS. *J. Neurosci.* **34**, 79–94 (2014).
19. Xiang, Z. et al. Input-specific regulation of glutamatergic synaptic transmission in the medial prefrontal cortex by mGlu2/mGlu4 receptor heterodimers. *Sci. Signal.* **14**, eabd2319 (2021).
20. Lin, X. et al. Differential activity of mGlu7 allosteric modulators provides evidence for mGlu7/8 heterodimers at hippocampal Schaffer collateral-CA1 synapses. *J. Biol. Chem.* **298**, 102458 (2022).
21. Kammermeier, P. J. Functional and pharmacological characteristics of metabotropic glutamate receptors 2/4 heterodimers. *Mol. Pharmacol.* **82**, 438–447 (2012).
22. Bennouar, K.-E. et al. Synergy between L-DOPA and a novel positive allosteric modulator of metabotropic glutamate receptor 4: implications for Parkinson's disease treatment and dyskinesia. *Neuropharmacology* **66**, 158–169 (2013).
23. Marino, M. J. et al. Allosteric modulation of group III metabotropic glutamate receptor 4: a potential approach to Parkinson's disease treatment. *Proc. Natl. Acad. Sci. USA* **100**, 13668–13673 (2003).
24. Hopkins, C. R., Lindsley, C. W. & Niswender, C. M. mGluR4-positive allosteric modulation as potential treatment for Parkinson's disease. *Future Med. Chem.* **1**, 501–513 (2009).
25. Urizar, E. et al. CODA-RET reveals functional selectivity as a result of GPCR heteromerization. *Nat. Chem. Biol.* **7**, 624–630 (2011).
26. Paulmurugan, R., Umezawa, Y. & Gambhir, S. S. Noninvasive imaging of protein-protein interactions in living subjects by using reporter protein complementation and reconstitution strategies. *Proc. Natl. Acad. Sci. USA* **99**, 15608–15613 (2002).
27. Lund, C. H. et al. A reversible Renilla luciferase protein complementation assay for rapid identification of protein-protein interactions reveals the existence of an interaction network involved in xyloglucan biosynthesis in the plant Golgi apparatus. *J. Exp. Bot.* **66**, 85–97 (2015).
28. Niswender, C. M. et al. Discovery, characterization, and antiparkinsonian effect of novel positive allosteric modulators of metabotropic glutamate receptor 4. *Mol. Pharmacol.* **74**, 1345–1358 (2008).
29. Maj, M. et al. (-)-PHCCC, a positive allosteric modulator of mGluR4: characterization, mechanism of action, and neuroprotection. *Neuropharmacology* **45**, 895–906 (2003).
30. Rovira, X. et al. Overlapping binding sites drive allosteric agonism and positive cooperativity in type 4 metabotropic glutamate receptors. *FASEB J.* **29**, 116–130 (2015).
31. Lin, S. et al. Structures of Gi-bound metabotropic glutamate receptors mGlu2 and mGlu4. *Nature* **594**, 583–588 (2021).
32. Isberg, V. et al. Generic GPCR residue numbers - aligning topology maps while minding the gaps. *Trends Pharmacol. Sci.* **36**, 22–31 (2015).
33. Engers, D. W. et al. Discovery, synthesis, and structure-activity relationship development of a series of N-(4-acetamido)phenylpicolinamides as positive allosteric modulators of metabotropic glutamate receptor 4 (mGlu(4)) with CNS exposure in rats. *J. Med. Chem.* **54**, 1106–1110 (2011).
34. Brock, C. et al. Activation of a dimeric metabotropic glutamate receptor by intersubunit rearrangement. *J. Biol. Chem.* **282**, 33000–33008 (2007).

35. Hampson, D. R. et al. Probing the ligand-binding domain of the mGluR4 subtype of metabotropic glutamate receptor. *J. Biol. Chem.* **274**, 33488–33495 (1999).
36. Wellendorph, P. & Bräuner-Osborne, H. Molecular basis for amino acid sensing by family C G-protein-coupled receptors. *Br. J. Pharmacol.* **156**, 869–884 (2009).
37. Francesconi, A. & Duvoisin, R. M. Role of the second and third intracellular loops of metabotropic glutamate receptors in mediating dual signal transduction activation. *J. Biol. Chem.* **273**, 5615–5624 (1998).
38. Chang, W., Chen, T. H., Pratt, S. & Shoback, D. Amino acids in the second and third intracellular loops of the parathyroid Ca2+-sensing receptor mediate efficient coupling to phospholipase C. *J. Biol. Chem.* **275**, 19955–19963 (2000).
39. Bräuner-Osborne, H. & Krogsgaard-Larsen, P. Pharmacology of (S)-homoquisqualic acid and (S)–2-amino-5-phosphonopentanoic acid [(S)-AP5] at cloned metabotropic glutamate receptors. *Br. J. Pharmacol.* **123**, 269–274 (1998).
40. Gusach, A., García-Nafría, J. & Tate, C. G. New insights into GPCR coupling and dimerisation from cryo-EM structures. *Curr. Opin. Struct. Biol.* **80**, 102574 (2023).
41. Seven, A. B. et al. G-protein activation by a metabotropic glutamate receptor. *Nature* **595**, 450–454 (2021).
42. Kniazeff, J. et al. Closed state of both binding domains of homodimeric mGlu receptors is required for full activity. *Nat. Struct. Mol. Biol.* **11**, 706–713 (2004).
43. Utley, T. et al. Synthesis and SAR of a novel metabotropic glutamate receptor 4 (mGlu4) antagonist: unexpected "molecular switch" from a closely related mGlu4 positive allosteric modulator. *Bioorg. Med. Chem. Lett.* **21**, 6955–6959 (2011).
44. Galici, R. et al. Biphenyl-indanone A, a positive allosteric modulator of the metabotropic glutamate receptor subtype 2, has antipsychotic- and anxiolytic-like effects in mice. *J. Pharmacol. Exp. Ther.* **318**, 173–185 (2006).
45. Schaffhauser, H. et al. Pharmacological characterization and identification of amino acids involved in the positive modulation of metabotropic glutamate receptor subtype 2. *Mol. Pharmacol.* **64**, 798–810 (2003).
46. Johnson, M. P. et al. Discovery of allosteric potentiators for the metabotropic glutamate 2 receptor: synthesis and subtype selectivity of N-(4-(2-methoxyphenoxy)phenyl)-N-(2,2,2- trifluoroethylsulfonyl)pyrid-3-ylmethylamine. *J. Med. Chem.* **46**, 3189–3192 (2003).
47. Jiang, L. I. et al. Use of a cAMP BRET sensor to characterize a novel regulation of cAMP by the sphingosine 1-phosphate/G13 pathway. *J. Biol. Chem.* **282**, 10576–10584 (2007).
48. Flor, P. J. et al. Molecular cloning, functional expression and pharmacological characterization of the human metabotropic glutamate receptor type 2. *Eur. J. Neurosci.* **7**, 622–629 (1995).
49. Hayashi, Y. et al. Role of a metabotropic glutamate receptor in synaptic modulation in the accessory olfactory bulb. *Nature* **366**, 687–690 (1993).
50. Wang, X. et al. Structural insights into dimerization and activation of the mGlu2-mGlu3 and mGlu2-mGlu4 heterodimers. *Cell Res.* **33**, 762–774 (2023).
51. Liu, L. et al. Asymmetric activation of dimeric GABAB and metabotropic glutamate receptors. *Am. J. Physiol. Cell Physiol.* **325**, C79–C89 (2023).
52. Du, J. et al. Structures of human mGlu2 and mGlu7 homo- and heterodimers. *Nature* **594**, 589–593 (2021).
53. Shaye, H. et al. Structural basis of the activation of a metabotropic GABA receptor. *Nature* **584**, 298–303 (2020).
54. Gao, Y. et al. Asymmetric activation of the calcium-sensing receptor homodimer. *Nature* **595**, 455–459 (2021).
55. Park, J. et al. Symmetric activation and modulation of the human calcium-sensing receptor. *Proc. Natl. Acad. Sci. USA* **118**, e2115849118 (2021).
56. Liu, J. et al. Allosteric control of an asymmetric transduction in a G protein-coupled receptor heterodimer. *Elife* **6**, e26985 (2017).
57. Park, J. et al. Structure of human GABAB receptor in an inactive state. *Nature* **584**, 304–309 (2020).
58. Papasergi-Scott, M. M. et al. Structures of metabotropic GABAB receptor. *Nature* **584**, 310–314 (2020).
59. Belkacemi, K., Rondard, P., Pin, J.-P. & Prézeau, L. Heterodimers revolutionize the field of metabotropic glutamate receptors. *Neuroscience* **S0306-4522**, 00270–00277 (2024).
60. Ellaithy, A., Gonzalez-Maeso, J., Logothetis, D. A. & Levitz, J. Structural and biophysical mechanisms of class C G protein-coupled receptor function. *Trends Biochem. Sci.* **45**, 1049–1064 (2020).
61. Asher, W. B. *et al*. *G-Protein-Coupled Receptor Dimers* (eds. Herrick-Davis, K., Milligan, G. & Di Giovanni, G.) 99–127 (Springer International Publishing, 2017).
62. Dale, N. C., Johnstone, E. K. M. & Pfleger, K. D. G. GPCR heteromers: an overview of their classification, function and physiological relevance. *Front. Endocrinol.* **13**, 931573 (2022).
63. Engers, D. W. et al. Discovery, synthesis, and preclinical characterization of N-(3-chloro-4-fluorophenyl)–1H-pyrazolo[4,3-b]pyridin-3-amine (VU0418506), a novel positive allosteric modulator of the metabotropic glutamate receptor 4 (mGlu4). *ACS Chem. Neurosci.* **7**, 1192–1200 (2016).
64. Yin, S., Zamorano, R., Conn, P. J. & Niswender, C. M. Functional selectivity induced by $mGlu_4$ receptor positive allosteric modulation and concomitant activation of Gq coupled receptors. *Neuropharmacology* **66**, 122–132 (2013).
65. Christov, C. et al. Integrated synthetic, pharmacological, and computational investigation of cis-2-(3,5-dichlorophenylcarbamoyl) cyclohexanecarboxylic acid enantiomers as positive allosteric modulators of metabotropic glutamate receptor subtype 4. *ChemMedChem* **6**, 131–140 (2011).

Acknowledgements

This work was supported by National Institutes of Health grants R01 NS132060 (J.A.J), R21NS113614 (J.A.J), R01 MH054137 (J.A.J), the Hope for Depression Research Foundation (J.A.J.), and Miriam's Magical Memorial Mission (J.A.J.). We thank P. Jeffrey Conn for helpful discussions related to the work as well as early support for the project from R01 NS031373. We also thank Qing R. Fan and Hao Zuo for reading the manuscript and for providing valuable insights regarding class C receptor structural activation.

Author contributions

X.L. prepared an initial draft of the manuscript, and W.B.A. and J.A.J. wrote the final manuscript, with contributions from all the authors. X.L., W.B.A., and J.A.J. designed the live-cell assays and interpreted the results with critical input from C.N. X.L. performed the live-cell CODA-RET and cAMP assays. D.P. designed and performed the binding pocket recognition and molecular docking simulations and the corresponding analysis. W.B.A. and J.A.J. supervised the project.

Competing interests

C.N. has received research support from Boehringer Ingelheim and Acadia Pharmaceuticals and has an equity interest in Appello Pharmaceuticals. The Boehringer Ingelheim and Acadia programs are focused on distinct targets to those explored here. Appello Pharmaceuticals licensed an $mGlu_4$ PAM from Vanderbilt, but the $mGlu_4$ compounds used in this paper are all in the public domain. The remaining authors declare no competing interests.

Additional information

Supplementary information The online version contains supplementary material available at https://doi.org/10.1038/s41467-024-52822-4.

Correspondence and requests for materials should be addressed to Wesley B. Asher or Jonathan A. Javitch.

Peer review information *Nature Communications* thanks Shane Hellyer, Jacob Piehler and the other, anonymous, reviewer(s) for their contribution to the peer review of this work. A peer review file is available.